Contract No:

This document was prepared in conjunction with work accomplished under Contract No. DE-AC09-08SR22470 with the U.S. Department of Energy (DOE) Office of Environmental Management (EM).

Disclaimer:

This work was prepared under an agreement with and funded by the U.S. Government. Neither the U. S. Government or its employees, nor any of its contractors, subcontractors or their employees, makes any express or implied:

1) warranty or assumes any legal liability for the accuracy, completeness, or for the use or results of such use of any information, product, or process disclosed; or
2) representation that such use or results of such use would not infringe privately owned rights; or
3) endorsement or recommendation of any specifically identified commercial product, process, or service.

Any views and opinions of authors expressed in this work do not necessarily state or reflect those of the United States Government, or its contractors, or subcontractors.

Porous Iron Oxide Nanorods and Their Photothermal Applications

George Larsen[1]*, Weijie Huang[2], Yiping Zhao[2], and Simona E. Hunyadi Murph[1,2**]

[1]National Security Directorate, Savannah River National Laboratory, Aiken, SC USA
[2]Department of Physics and Astronomy, The University of Georgia, Athens, GA, USA
*George.Larsen@srnl.doe.gov
**Simona.Murph@srnl.doe.gov

ABSTRACT

Iron oxide is a unique semiconductor material, either as a single nanoparticle, or as a component of multifunctional nanoparticles. Its desirable properties, abundance, non-toxicity, and excellent magnetic properties make it a valuable for many applications. Porous iron oxide nanorods are able to transduce light into heat through the photothermal effect. Photothermal heating arises from the energy dissipated during light absorption leading to rapid temperature rise in close proximity to the surface of the nanoparticle. The heating effect can be efficiently harnessed to drive/promote different physical phenomena. In this report, we describe the synthesis and properties of porous Fe_3O_4 for photothermal applications. We then demonstrate their use as photothermally enhanced and recyclable materials for environmental remediation through sorption processes.

KEYWORDS: Photothermal, iron oxide, Fe_3O_4, magnetite, adsorption, methylene blue, co-deposition, oblique angle deposition, nanorods

1. INTRODUCTION

The magnetite phase of iron oxide, or Fe_3O_4, is an abundant, non-toxic, conductive semimetallic semiconductor with a band gap of 0.2 eV [1]. These properties are attractive from an economic standpoint, but technological applications of bulk iron oxides are generally limited due to their relatively unremarkable properties. However, recent research has shown that at the nanoscale, iron oxide exhibits new or enhanced properties when compared to their bulk form, and therefore, have enabled new applications. For example, iron oxide nanomaterials have been used as catalysts, photocatalysts, and as chemical sensors [2-4]. Notably, magnetite particles also have magnetic properties. Fe_3O_4 is ferrimagnetic in the bulk form, but nanoparticles can also exhibit superparamagnetism [5]. Fe_3O_4 nanostructures have also generated significant interest due to their size and shape-dependent magnetic properties and have been used in such applications as magnetic sensors [6], ferrofluids [7], magnetic resonance imaging (MRI) contrast agents [8], drug delivery vessels [9], and magnetic hyperthermia [10].

An interesting property of Fe_3O_4 nanoparticles is its ability to transduce light into heat through the photothermal effect [11]. Photothermal heating arises from the energy dissipated during light absorption by the nanoparticle. An important aspect of the photothermal heating is the rapid temperature rise in close proximity to the surface of the nanoparticle. For a collection of nanoparticles, a significant large scale temperature increase can be observed within minutes due to collective thermal effects [12]. This heating effect is efficient and can be harnessed to facilitate different physical phenomena. In this report, we describe the synthesis and properties of porous Fe_3O_4 nanorods. Subsequently, these nanoparticles were evaluated as sorption materials for environmental applications by exploiting their photothermal properties.

2. EXPERIMENTAL SECTION

2.1 Porous Fe_3O_4 nanorod fabrication

The magnetic porous Fe_3O_4 nanorods were fabricated by the oblique angle co-deposition technique [13]. First, a monolayer made of 500 nm diameter SiO_2 beads was coated on Si substrate, which serves as a deposition template using a reported method [14]. The bead-coated substrates were then loaded into a custom built co-resources electron beam evaporation deposition chamber. Fe_2O_3 and Ag were simultaneously deposited onto the monolayers at a vapor incident angle of 86° and at a rate of ~ 0.1 nm/s and 0.05 nm/s, respectively. The deposition rates were separately monitored by two quartz crystal microbalances (QCM) facing directly toward the incident vapor. The deposition was stopped when the combined QCM reading reached 2 μm. The as-deposited samples were then annealed in ethanol/nitrogen environment at 350 °C for 1 hour in order to reduce Fe_2O_3 to Fe_3O_4. To obtain the porous Fe_3O_4 nanorods, the Ag atoms in the nanorods are gradually etched using 0.05 M KCN (Fischer Scientific, ACS grade) in 99.9% pure methanol (ACS grade) solvent. The samples were then washed in the distilled water and absolute ethanol for several times to remove any impurities before characterization.

2.2 Photothermal heating experiments:

The photothermal experimental setup consists of a laser with wavelength λ = 532 nm (Del Mar Photonics, DMPV-532-1, beam diameter focused to ~20 μm at 1200 mW), where the beam path is directed onto the top surface of 3 mL nanoparticle solution contained in a methacrylate cuvette [15]. The cuvette is resting on scale (Mettler Toledo XP205) that provides dynamic mass measurements. These data are synchronized with the bulk solution temperature data, which is obtained from an infrared thermocouple (Omega Engineering, OS801-HT). The data is logged using a custom LabVIEW program.

2.3 Photothermal desorption experiment

3 mL of a 30 μM methylene blue (MB) solution was placed in a cuvette containing a porous Fe_3O_4 nanorod array on Si wafer (~1 cm^2). The sorption of MB onto the porous Fe_3O_4 nanorod array was measured by monitoring the absorbance of the MB solution through the sides of the cuvette every 30 minutes for 2 hours. For the dark experiment, the MB@Fe_3O_4 nanorod array is rinsed in a stream of DI water, and placed in a clean cuvette with 3 mL of DI water. The cuvette is placed in the dark, and the absorbance of the solution was measured through the sides of the cuvette after 30 minutes and 1 hour. After the dark experiment, the MB@Fe_3O_4 NR array is illuminated using the photothermal setup described in Section 2.3. The absorbance of the solution was measured through the sides of the cuvette every few minutes.

3. RESULTS AND DISCUSSION

3.1 Morphology and optical properties

As described above in Section 2.1, the porous Fe_3O_4 nanorods are first fabricated by co-depositing Ag and Fe_2O_3 onto a SiO_2 template in a vacuum deposition system, to create Ag-Fe_2O_3 nanorods. The Fe_2O_3 is converted to Fe_3O_4 by annealing in a reducing atmosphere, creating aligned arrays of Ag- Fe_3O_4 nanorods. A representative scanning electron microscopy (SEM) image of these nanorods is shown in **Figure 1a**. The obtained nanorods have a featherlike morphology, and the smaller brighter Ag nanoparticles can be seen dispersed on and within the supporting Fe_3O_4 nanorods. The Fe_3O_4 nanorods are approximately 1 um in length and have diameters around 300 nm, while the interspersed Ag nanoparticles have a range of sizes up to around 100 nm. In order to create the porous Fe_3O_4 nanorods, the spherical Ag nanoparticles in the Ag- Fe_3O_4 nanorods are gradually removed over 60 minutes using a methanol-KCN etchant. **Figure 1b** shows an SEM image of the porous Fe_3O_4 nanorods. As can be seen in the image, the morphology of the nanorods changes considerably after etching. The surface becomes significantly rougher with a "sponge-like" appearance. The original Fe_3O_4 nanorod framework remains intact even after the Ag nanosphere dissolution. Interconnected hierarchical layers of Fe_3O_4 with hollow openings (pores) can be seen throughout the nanorod volume.

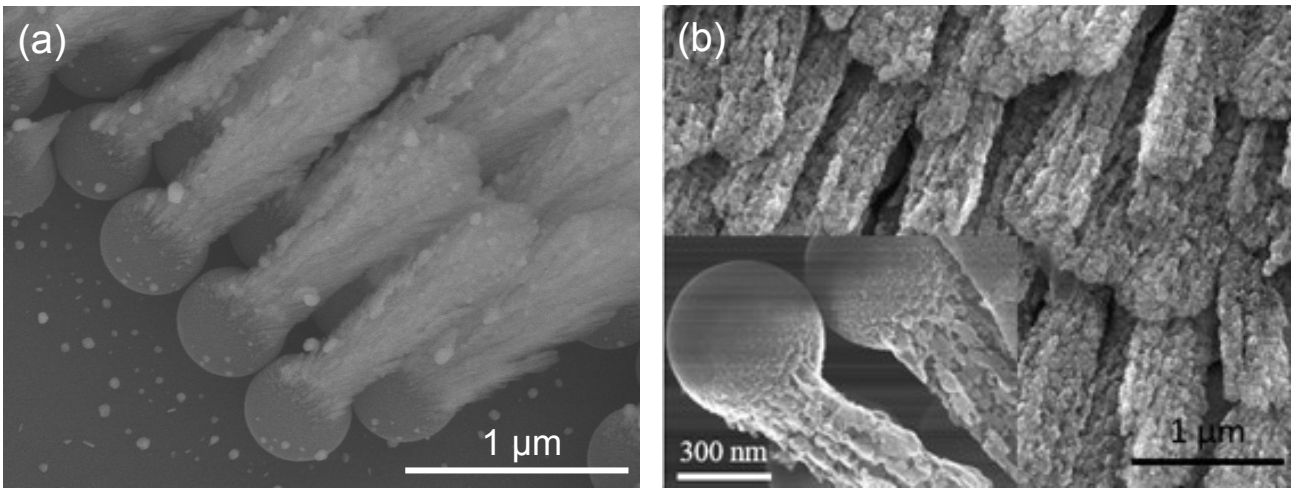

Figure 1. (a)Scanning electron microscopy (SEM) image of the Ag-Fe_3O_4 nanorod array. (b) SEM image of the porous Fe_3O_4 nanorod array obtained by etching the Ag out of the nanorods seen in Fig. 1a. The inset shows a higher magnification image of the porous Fe_3O_4 nanorod morphology. The large spheres in the images are the SiO_2 beads, which are used as templates for the nanorod fabrication.

Since the pores are related to the original shape and size of the dispersed Ag nanoparticles, the pores have a range of different sizes up to 100 nm in diameter.

Figure 2 shows the UV-vis-NIR absorbance spectrum of porous Fe_3O_4 nanorods dispersed in deionized water. The spectrum is broadband and mostly featureless. The magnitude of absorbance gradually increases for decreasing wavelengths over λ = 300 - 1000 nm. The spectrum is consistent with the behavior of dispersed nanoparticles exhibiting non-resonant absorbance and scattering of light [16]. The increased absorbance over the visible region (λ = 400 - 700 nm), makes these nanoparticles useful for applications which harness ambient light sources, such as solar energy.

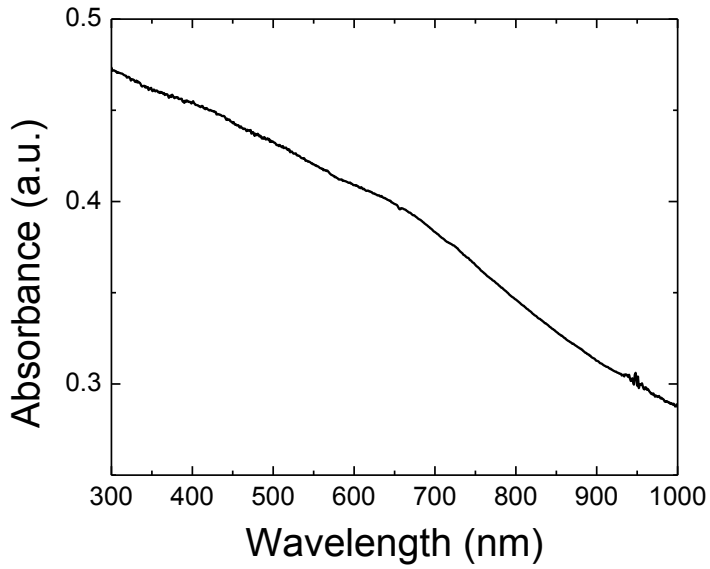

Figure 2. (a) UV-vis-NIR absorbance spectrum of porous Fe_3O_4 nanorods dispersed in deionized water.

3.2 Photothermal heating

As described above, light absorption in materials can be readily dissipated as heat. Nanoparticles, in particular, can generate a significant amount of heat and increase temperatures in their vicinities due to their large absorbance cross-sections [11]. The amount of heat generated by single nanoparticle is directly related to the amount of light that is absorbed by that nanoparticle, which can be measured experimentally or calculated from electromagnetic theory or by simulation [17-19]. According to theory, the photothermally-induced temperature rise of a single, isolated nanoparticle under most illumination conditions may only be on the order 0.06 °C [12]. However, if a sufficient number of nanoparticles are illuminated, the temperature fields of all of the nanoparticles overlap and create a substantial global temperature rise [20].

Figure 3a shows the temperature rise of laser-illuminated solutions of pure water and porous Fe_3O_4 nanorods dispersed in deionized water. For the porous Fe_3O_4 nanorods solutions, a noticeable increase in temperature is observed within a few seconds after the laser is turned on. The temperature increases exponentially and approaches a limiting value until the laser is turned off. This behavior is consistent with heat diffusion occurring in a dissipative medium [17]. The maximum solution temperature achieved during the experiment is T_{max} = 61 ºC. The control experiment with laser illuminated pure DI water shows no perceptible temperature rise, indicating that the photothermal heating seen for the nanorods is a nanoparticle-mediated effect. **Figure 3b** shows the mass loss, Δm, of the different solutions during the photothermal heating experiment. The control experiment of pure DI water is indicative of the background evaporation rate, which is unaffected by the laser. In comparison, the porous Fe_3O_4 nanorods show a much larger change in mass under illumination, indicating that the laser light produces a larger amount of water vapor during photothermal heating.

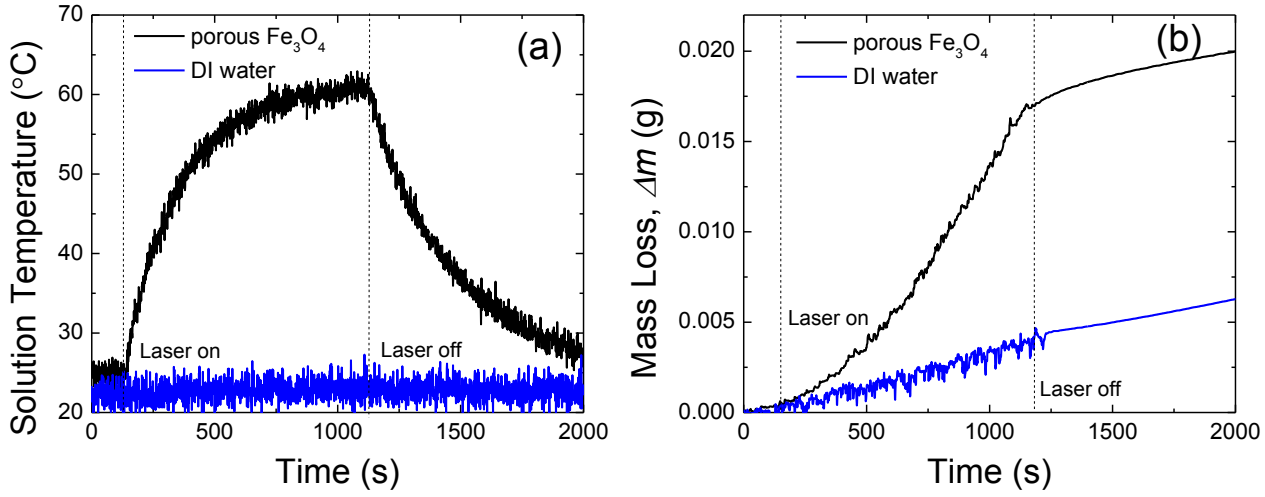

Figure 3. (a) Temperature rise of solution during photothermal heating of dispersed porous Fe_3O_4 nanorods with a laser, λ = 532 nm. The temperature profile of the control experiment, laser illuminated DI water, is also shown. (b) Mass loss of the solution for dispersed porous Fe_3O_4 nanorods and for pure water during photothermal experiments.

3.3. Photothermal desorption

The removal of dyes from industrial wastewater is a concern due to their widespread use and the fact that many dyes are non-biodegradable and toxic. The removal or destruction of methylene blue dye (MB) has become a benchmark test for different sorbents and photocatalysts in the literature [21]. This is because the loss of MB is easily monitored by its absorbance peak at λ = 664 nm. Dye removal via adsorption onto sorbent media is faster, easier, and more economic than photocatalytic destruction, and is therefore, the industrially preferred method [22]. However, additional

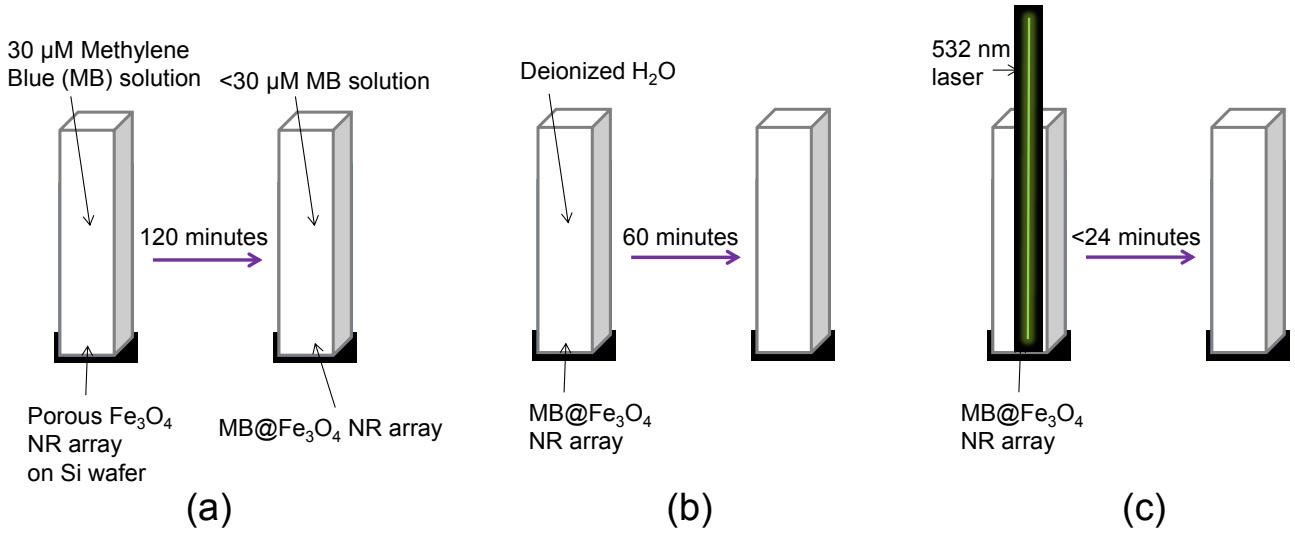

Figure 4. Schematics depicting the different steps of the photothermal experiment: (a) Step 1 - methylene blue (MB) is adsorbed onto porous Fe_3O_4 nanorod arrays by incubating them in a 30 μM MB solution; (b) Step 2 - MB coated porous Fe_3O_4 nanorod arrays are rinsed then placed in pure water for 60 minutes to check for dark desorption; (c) Step 3 - the MB coated porous Fe_3O_4 nanorod arrays in pure water are illuminated with a laser (λ = 532 nm) and MB desorbs from the nanorod surface due to photothermal heating.

improvements in cost and efficiency could be obtained if the sorbent material was regenerable. Since sorption is a thermodynamically driven process, photothermal heating offers a route to remotely moderate the sorption of materials.

In order to investigate the effect of photothermal heating on dye sorption, porous Fe_3O_4 nanorods, supported on a Si wafer, were fabricated as described in Section 2.2. These porous Fe_3O_4 nanorods were loaded with MB dye by incubating in 30 μM solution for 2 hours (**Figure 4**, also see Section 2.3 for experimental details). During the loading experiment, the UV-vis absorbance of the MB solution decreased, indicating capture of the dye molecules by the porous nanorods (**Figure 5a**). After MB loading, the nanorods were rinsed and placed in a clean cuvette containing only DI water. If left in the dark, only trace amounts of MB molecules desorb from the porous Fe_3O_4 nanorods into the DI water after one hour incubation (**Figure 5b**). On the other hand, when the porous Fe_3O_4 nanorods are illuminated with a laser (λ = 532 nm), MB molecules rapidly desorb from the nanorods, as indicated by the appearance of the MB peaks in the UV-vis spectra (**Figure 5c**). During the photothermal heating experiment, the solution temperatures gradually increase from T = 24 °C to T = 47 °C, as measured by the IR thermocouples. The amount of dye released can be quantified by integrating the spectra shown in **Figure 5c** over λ = 550 – 700 nm. The plot of the integrated area versus time is shown in **Figure 5d**. It can be seen that the MB peak area initially increase rapidly, but after ~ 10 minutes the MB peak area decreases, possibly due to photolysis, photocatalysis, photobleaching, or a combination of those. Thus, the porous Fe_3O_4 nanorods combined with photothermal heating offers a route to remotely capture and release harmful molecules in a controlled manner. While this experiment was conducted using laser light, more scalable illumination sources, such as the sun or LEDs could be used to make the process industrially relevant.

4. CONCLUSION

This report describes the synthesis and fabrication of porous Fe_3O_4 nanorods. It was shown that this nanostructure is capable of transducing heat from light and can generate significant temperature increases in surrounding solutions. Furthermore, this photothermal heating effect can be employed to improve chemical processes or remotely control some

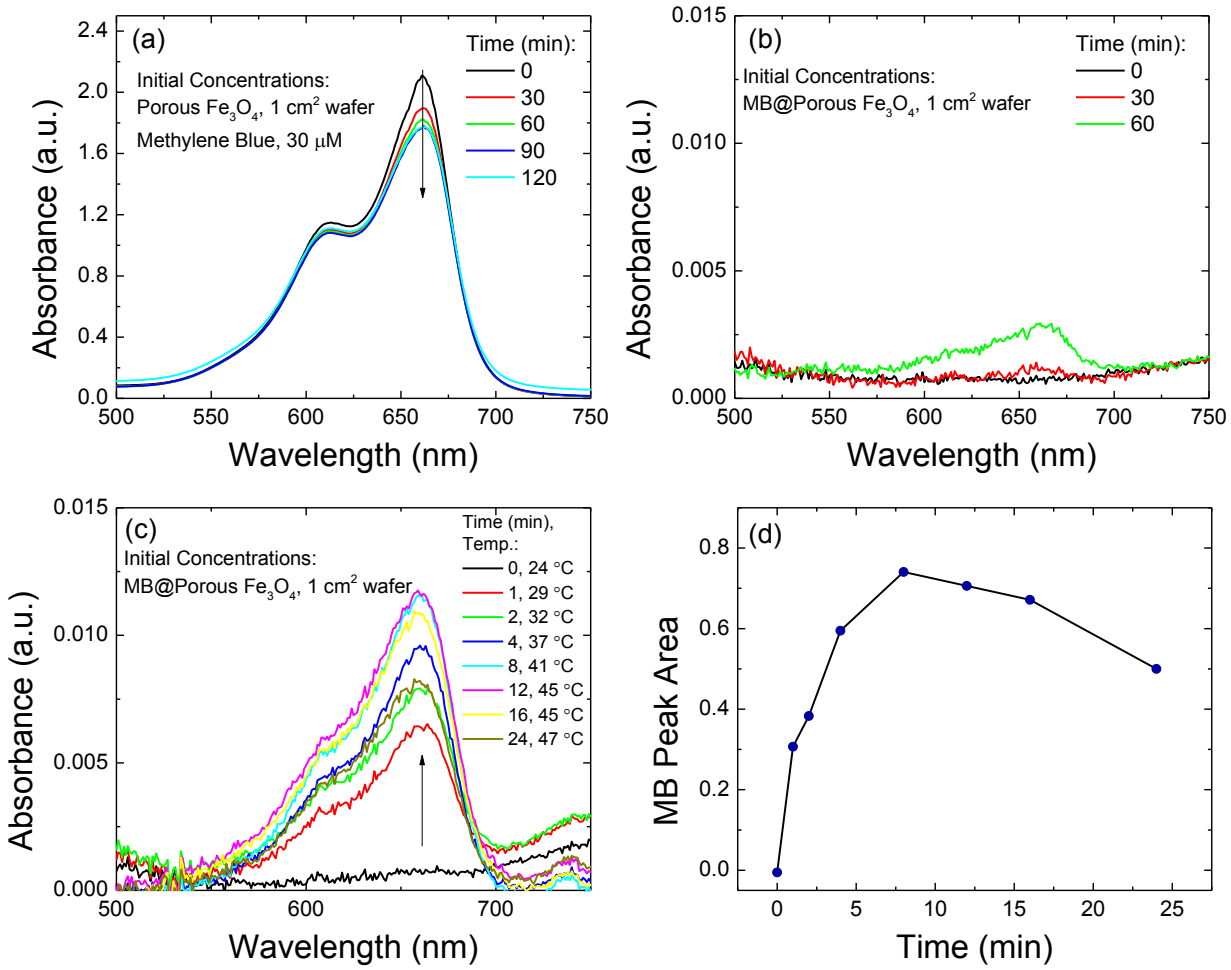

Figure 5. (a) UV-vis monitoring of methylene blue (MB) adsorption onto porous Fe_3O_4 nanorod arrays. The MB absorbance peak values decrease as MB is adsorbed onto the nanorods. (b) Dark desorption experiment spectra: MB coated porous Fe_3O_4 nanorod arrays are placed in pure water. Slight MB peaks emerge over time as trace amounts desorb from the nanorod surfaces. (c) Photothermal desorption experiment spectra: the MB coated porous Fe_3O_4 nanorod arrays in pure water are illuminated with a laser and the MB absorbance peaks rapidly emerge as the MB desorbs from the nanorod surface due to photothermal heating. (d) Integrated MB peak area versus time for the photothermal desorption experiment.

thermodynamic phenomenon. In the case above, we have demonstrated that the sorption of methylene blue molecules onto porous Fe_3O_4 nanorods can be remotely controlled by laser irradiation. While this application is related to wastewater treatment, the photothermal effects of iron oxide based nanoparticles could readily extend beyond environmental remediation. The magnetic properties and biocompatibility of Fe_3O_4 is desirable for biomedical applications, in particular. For example, the porous Fe_3O_4 nanorods could be loaded with pharmaceuticals instead of dye molecules, creating a MRI contrast agent that could provide remotely targeted therapeutics. Given their unique properties and low cost, the use of iron-oxide for photothermal applications could have significant impact in other fields as well.

Acknowledgements: The financial support of this work was provided by Department of Energy DOE- Laboratory Directed Research & Development (LDRD) Strategic Initiative Program. We thank Dr. Robert Lascola for providing time and expertise to assist us with our experiments.

References:

1. Cornell, R. M. and Schwertmann, U., [Introduction to the Iron Oxides], Wiley-VCH Verlag GmbH & Co. KGaA, Weinheim, (2004).

2. Zeng, T., Chen, W.-W., Cirtiu, C. M., Moores, A., Song, G., and Li, C.-J., "Fe3O4 nanoparticles: a robust and magnetically recoverable catalyst for three-component coupling of aldehyde, alkyne and amine." Green Chem., 12(4), 570-573 (2010).

3. Kumar, B., Smita, K., Cumbal, L., Debut, A., Galeas, S., and Guerrero, V. H., "Phytosynthesis and photocatalytic activity of magnetite (Fe 3 O 4) nanoparticles using the Andean blackberry leaf." Mater. Chem. Phys., 179 310-315 (2016).

4. Zhang, Z., Zhu, H., Wang, X., and Yang, X., "Sensitive electrochemical sensor for hydrogen peroxide using Fe3O4 magnetic nanoparticles as a mimic for peroxidase." Microchim. Acta, 174(1-2), 183-189 (2011).

5. Xuan, S., Wang, Y.-X. J., Yu, J. C., and Cham-Fai Leung, K., "Tuning the grain size and particle size of superparamagnetic Fe3O4 microparticles." Chem. Mater., 21(21), 5079-5087 (2009).

6. Thakur, H. V., Nalawade, S. M., Gupta, S., Kitture, R., and Kale, S., "Photonic crystal fiber injected with Fe3O4 nanofluid for magnetic field detection." Appl. Phys. Lett., 99(16), 161101 (2011).

7. Parekh, K., Upadhyay, R., and Mehta, R., "Magnetic and rheological characterization of Fe3O4 ferrofluid: particle size effects." Hyperfine Interact., 160(1-4), 211-217 (2005).

8. Hu, F., Wei, L., Zhou, Z., Ran, Y., Li, Z., and Gao, M., "Preparation of biocompatible magnetite nanocrystals for in vivo magnetic resonance detection of cancer." Adv. Mater., 18(19), 2553-2556 (2006).

9. Cao, S.-W., Zhu, Y.-J., Ma, M.-Y., Li, L., and Zhang, L., "Hierarchically nanostructured magnetic hollow spheres of Fe3O4 and γ-Fe2O3: preparation and potential application in drug delivery." J. Phys. Chem. C, 112(6), 1851-1856 (2008).

10. Baker, I., Zeng, Q., Li, W., and Sullivan, C. R., "Heat deposition in iron oxide and iron nanoparticles for localized hyperthermia." J. Appl. Phys., 99(8), 08H106 (2006).

11. Govorov, A. O. and Richardson, H. H., "Generating heat with metal nanoparticles." Nano today, 2(1), 30-38 (2007).

12. Keblinski, P., Cahill, D. G., Bodapati, A., Sullivan, C. R., and Taton, T. A., "Limits of localized heating by electromagnetically excited nanoparticles." J. Appl. Phys., 100(5), 054305 (2006).

13. He, Y. and Zhao, Y., "Advanced multi-component nanostructures designed by dynamic shadowing growth." Nanoscale, 3(6), 2361-2375 (2011).

14. Larsen, G. K., He, Y., Ingram, W., and Zhao, Y., "Hidden Chirality in Superficially Racemic Patchy Silver Films." Nano Lett., 13(12), 6228-6232 (2013).

15. Murph, S. E. H., Larsen, G. K., and Lascola, R. J., "Multifunctional Hybrid Fe2O3-Au Nanoparticles for Efficient Plasmonic Heating." (108), e53598 (2016).

16. Bohren, C. F. and Huffman, D. R., [Absorption and Scattering by an Arbitrary Particle], Wiley-VCH Verlag GmbH, New York, (2007).

17. Jiang, K., Smith, D. A., and Pinchuk, A., "Size-dependent Photothermal conversion efficiencies of plasmonically heated gold nanoparticles." J. Phys. Chem. C, 117(51), 27073-27080 (2013).

18. Kelly, K. L., Coronado, E., Zhao, L. L., and Schatz, G. C., "The optical properties of metal nanoparticles: the influence of size, shape, and dielectric environment." J. Phys. Chem. B, 107(3), 668-677 (2003).

19. Larsen, G. K., Farr, W., and Hunyadi Murph, S. E., "Multifunctional Fe2O3–Au Nanoparticles with Different Shapes: Enhanced Catalysis, Photothermal Effects, and Magnetic Recyclability." J. Phys. Chem. C, 120(28), 15162-15172 (2016).

20. Govorov, A. O., Zhang, W., Skeini, T., Richardson, H., Lee, J., and Kotov, N. A., "Gold nanoparticle ensembles as heaters and actuators: melting and collective plasmon resonances." Nanoscale Res. Lett., 1(1), 84-90 (2006).

21. Houas, A., Lachheb, H., Ksibi, M., Elaloui, E., Guillard, C., and Herrmann, J.-M., "Photocatalytic degradation pathway of methylene blue in water." Appl. Catal., B, 31(2), 145-157 (2001).

22. Basnet, P. and Zhao, Y., "Superior dye adsorption capacity of amorphous WO 3 sub-micrometer rods fabricated by glancing angle deposition." J. Mater. Chem. A, 2(4), 911-914 (2014).